Scour Assessment of Bridge Foundations Using an *In Situ* Erosion Evaluation Probe (ISEEP)

M. Kayser[1] and M. A. Gabr[2]

[1]Graduate Research Assistant
Department of Civil, Construction and Environmental Engineering
North Carolina State University
Raleigh, NC 27695-7908
E-mail: mfkayser@ncsu.edu
Fax: 919-515-7908

[2]Professor, Ph.D., P.E.
Department of Civil, Construction and Environmental Engineering
North Carolina State University
Raleigh, NC 27695-7908
E-mail: gabr@eos.ncsu.edu
Phone: 919-515-7904
Fax: 919-515-7908

Submitted to: 92nd Transportation Research Board Annual Meeting,
January 13-17, 2013, Washington, D.C.

No. of text words = 5,500
Equivalent No. of words for figures = 6 (figures) × 250 = 1500
Equivalent No. of words for tables = 3 (tables) × 250 = 750
Total No. of words = 7,750

Scour Assessment of Bridge Foundations Using *In Situ* Erosion Evaluation Probe (ISEEP)

Abstract

Work in this paper presents the use of an *in situ* erosion evaluation probe (ISEEP) to assess scour depth at bridge piers. Numerical modeling and deployment of the device at a North Carolina Outer Banks site damaged by Hurricane Irene in 2011 demonstrates the applicability of the proposed concept. Computational fluid dynamics (CFD) software, FLOW-3D, is used to assess the scour depth at a bridge pier, and the results are compared against values that are based on ISEEP-estimated parameters using an excess stream power model. The scour depth is also calculated using empirical equations that assume the same conditions as those used in the numerical analysis. Parametric analysis using FLOW-3D indicates that among the parameters used for defining the scour depth, the entrainment coefficient (C_e) has the largest effect, whereas the drag coefficient (C_d) has the smallest effect within the range of values used in the analysis. The estimated scour depths that are based on ISEEP data agree relatively well with the scour magnitudes obtained from the numerical analysis, because the ISEEP data reflect the changes in properties of the sand layer in terms of depth. In contrast, the scour depth calculated from the empirical equations underestimated the scour depth, mainly because the equations have no provision for a layered soil profile. The use of ISEEP data, therefore, provides the advantage of an *in situ* assessment of the scour parameters because the properties of the soil layers vary according to depth. Further validation of both the field testing procedure and data reduction approach, including the assessment of the applicability of soils that contain an appreciable percentage of fines, is recommended.

INTRODUCTION

According to Lagasse et al. (*1*), there were 488,750 bridges over stream and river crossings in the United States with an annual cost for scour-related bridge failures estimated at $30 million. Furthermore, it was reported that more than 1,000 bridges have collapsed in the United States over the past thirty years, with about 60% of such failures caused by excess scour at the supporting foundation system (*2*). Therefore, the monitoring and assessment of scour potential and the determination of the erosion rate of the soils that support these structures are needed tasks during the design, operation, and lifetime of such hydraulic structures. In addition to being critical in the initial design phase, these erosion magnitude and rate data are also needed to develop maintenance priorities and establish replacement schedules.

Current techniques for assessing *in situ* erosion potential with depth require either the removal of soil samples for laboratory testing in a device such as the *Erosion Function Apparatus* (EFA), developed by Briaud et al. (*2*), or measuring only erosion that has already occurred by monitoring changes in the mud-line elevation with respect to time. The instruments used for these techniques range from simple steel sounding rods to remote sensing devices that employ electromagnetic waves and/or sonar with sound propagation. As shown by Lu et al. (*3*), sophisticated approaches, such as acoustic Doppler and ground penetration radar, are costly and require frequent maintenance and repair.

Hanson et al. (*4*) and Hanson and Cook (*5)* have reported the use of vertical jets for taking surface measurements of erosion potential in the field. These authors presented a framework for rendering stress that is caused by an impinging jet in the form of applied shear stress. In this case, a *potential core* is defined as the part of the jet where water retains its original

nozzle velocity. The jet deflects once it reaches the soil surface and therefore applies shear stress (τ) to the soil. This stress is expressed by Hanson and Cook (*5*) as:

$$\tau\ (N/m^2) = C_f \rho U_0^2 \quad (1)$$

where τ = applied shear stress to bed in N/m^2; U_0 = average velocity of water at the tip (m/s); ρ = density (kg/m^3); and C_f is the friction coefficient = 0.00416.

The rate of erosion is then estimated on the basis of excess shear, as presented by the Mehta model (*6*). Annandale (*7*) presented the concept of *stream power* as an estimate of the flow erosive potential and indicated that this concept is especially useful in the case of turbulent flow. Annandale noted that for jet testing, the flow is turbulent, and the input to the system is better represented by stream power, P, in watt per unit area, as follows (*7*):

$$P = \gamma qH, \text{ or in terms of shear stress, } P = \tau U_o \quad (2)$$

where P is in the unit of $watt/m^2$ (1 watt = 1 N.m per sec or $Kg.m^2$ per sec^3); γ = unit weight of water; q = discharge per unit area; H = energy head; and U_o = induced velocity. Furthermore, based on boundary layer theory, Annandale (*7*) recommended that the C_f parameter in Equation 1 is assumed to be 0.016.

Gabr et al. (*8*) presented a prototype device, termed *ISEEP* (*in situ* erosion evaluation probe) to assess soil erosion parameters in terms of depth. The concept draws from the approach taken by Hanson et al. (*4*) and utilizes the stream power concept introduced by Annandale (*7*) for the data reduction scheme. A prototype ISEEP has been constructed by attaching simple stainless steel tubes fitted with a truncated cone tip. The cone-tipped vertical probe is attached to a digitally controlled centrifugal pump that provides controllable and repeatable water velocity at the tip, with a sustained flow rate against any induced back pressure.

The critical stream power (P_c) and the soil detachment rate coefficient (k_d') values are assessed as the scour parameters based on ISEEP data. These two values (P_c and k_d') are used in conjunction with the applied stream power ($P_{applied}$) to compute the rate of erosion (E) in a fashion similar to the excess shear model, as follows (*7*):

$$E = k_d' (P_{applied} - P_c) \quad (3)$$

Based on the results from tests conducted in a sand pit (*8*), the measured parameters obtained from the probe testing are P_c = 20 $watt/m^2$ and k_d' = 0.0014 cm/sec per $watt/m^2$ for sand with D_{50} = 0.30 mm. The viability of obtaining various penetration rates using the probe with an increasing jet velocity is demonstrated in this work. Results also indicate that the probe is capable of applying various velocities with the same flow rate as well as various flow rates at the same velocity by changing the size of the jet orifice (*8*).

The issue of bridge pier scour also has been studied via laboratory flume tests, field tests, and numerical modeling using CFD models (*9-19*). Parameters such as stream velocity, depth of fluid and geometric dimensions of a given structure have been varied in the laboratory to simulate various site conditions (*9-12*). Melville and Coleman (*9*) have presented details about the mechanisms of local scour at bridge piers. Laursen and Toch (*10*), Shen et al. (*11*), and Melville and Sutherland (*12*) varied the depth of flow, stream velocity, angle of attack, pier

shape and grain size in laboratory flume to study scour depth at a bridge pier and developed empirical equation based on the laboratory results. Melville (*13*) also evaluated local scour at bridge piers by performing field tests at four different sites, and considered flow depth, flow velocity, pier shape and sediment size as variables. Scour depth measurements obtained in the field matched reasonably well with the empirical equation proposed by Shen et al. (*11*). Richardson and Davis (*14*) also recommended equations that they developed from the results of an experimental study and that are currently implemented in Hydraulic Engineering Circular No. 18 (HEC-18). Mueller (*15*) used 224 measurements of scour at 90 bridge piers in the United States, and compared the results from 22 scour empirical equations and recommended the use of HEC-18 equation for assessment of scour at bridge piers. In addition to the experimental studies, flow around circular pier has been simulated by several researchers (*16-19*) using different CFD models.

Work in this paper presents a case study for the assessment of scour potential with depth using ISEEP data. Field tests were conducted at the North Carolina Outer Banks at the site of a breach that occurred during Hurricane Irene in August 2011, where a temporary bridge is now installed. The soil detachment rate coefficient (k_d') and critical stream power (P_c) are evaluated based on the field data. CFD software, FLOW-3D, is used to perform the numerical simulations of the scour magnitude at the pier foundation, and the results are compared with those computed based on the ISEEP data. A parametric study is performed to illustrate the applicability of the data collected from the ISEEP in terms of the magnitude of scour computed using the numerical approach. Results based on the ISEEP data are also compared with scour depth estimated from empirical equations reported in the literature for assessing local scour at bridge piers.

FIELD TESTING

Field tests were conducted at a site along NC-12 that was breached during Hurricane Irene in 2011. Flooding from the hurricane rain eroded a 274 m section of NC-12 within the Pea Island National Wildlife Refuge. This rain erosion was caused by high water backwash from the sound side of the island. The maximum depth of the breach was estimated to be approximately 4 m with flow velocities ranging from 0.5 to 1 m/sec, with some instances of flow velocities as high as 4 m/s (*20*). An estimated erosion rate of up to 4 m/hr, with even higher rates occurring in a narrow window of less than 2 hours, was used for the site-based modeling (*20*). Repairs to render NC-12 operational consisted of building a temporary bridge approximately 200 m long. The two-lane bridge is founded on 12 footings (bents) supported by 82 piles. This bridge is a temporary solution (but is expected to function for several years) until a permanent one is implemented.

Figure 1 shows a photograph of the breach location with the temporary bridge installed and the ISEEP set-up in the field. Samples for the grain size distribution were collected from the soil that washed out of the hole during ISEEP testing. The first patch sample was collected from a depth down to approximately 0.5 m, and the second patch from a depth between 0.5 m and 1.5 m. As shown in Figure 2, the test soil at the site has a D_{50} = 0.32 mm with some of the shallower samples containing organic materials and shells that indicate an even coarser distribution.

The test procedure follows that described by Gabr et al. (*8*). In order to estimate the critical stream power (P_c) at two different depths, the penetration rate is plotted against the natural log of the stream power, and extrapolation is performed to a zero penetration rate, as shown in Figure 3. In the depth range of 0-0.5 m, the P_c value is 200 watt/m^2, and drops to 42 watt/m^2 after 0.5 m within the test depth. The road was severely damaged at this location where an inlet opened up. The uncorrected N values, below the debris of the pavement material,

decrease from 20 near the surface to 6 at 4.6 m and then to weight of hammer at 6 m (NCDOT 2011 boring log). The values of k_d', obtained using best fit linear interpolation, are 0.0009 and 0.001 cm/s per watt/m^2 for the two depth ranges, respectively.

(a) (b)

FIGURE 1. (a) Temporary bridge along NC-12, and (b) ISEEP set-up for field testing.

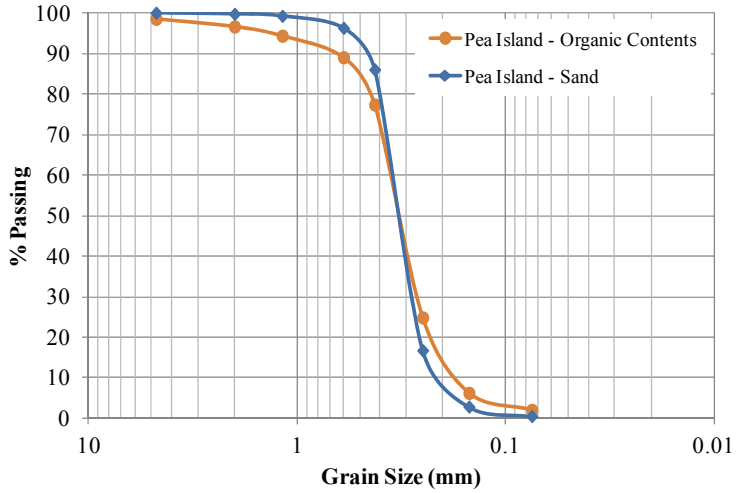

FIGURE 2. Grain size distribution of test site: Pea Island.

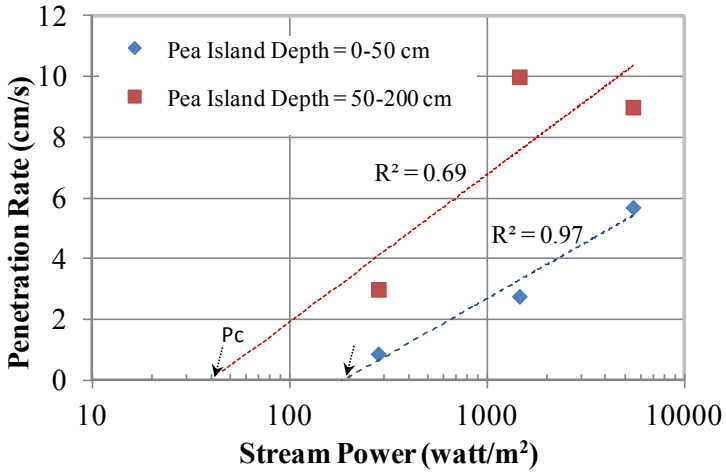

FIGURE 3. Extrapolation to estimate critical value of stream power at the onset of erosion.

NUMERICAL MODELING

The CFD software, FLOW-3D, is used to perform numerical simulations of scour at bridge piers. FLOW-3D (*21*) is based on the fundamental laws of mass, momentum and energy conservation. It simulates the flow process using the standard Navier-Stokes flow equation. The domain is discretized using finite difference blocks, and the governing equation is solved for each computational cell. The fractional area-volume obstacle representation (FAVOR) method is utilized for modeling solid obstacles within the domain (*22*).

Scour Model

A sediment scour turbulence model can be used to simulate the scour around a cylindrical bridge pier. According to Brethour and Burnham (*23*), the sediment scour model can simulate the deposition and entrainment of sand, silt and other non-cohesive soils as suspended and packed sediment. According to FLOW-3D (*21*), suspended sediments are typically of low concentration and advect with fluid. Packed sediments exist in the computational domain at the critical packing fraction, as defined by the user. The input parameters of the sediment scour model are: diameter and density of the sediment species (d, ρ), the critical Shields parameter, drag coefficient (C_d), entrainment coefficient (C_e), bed load coefficient (C_b) and angle of repose (ϕ). When the critical Shields parameter is not assigned during the numerical simulation, FLOW-3D calculates the value from the Shields curve (*23*). The definitions of C_e, C_d, and C_b are as follows:

i. C_e describes the lifting of the sediment in the bulk flow of fluid. According to FLOW-3D (*21*), the entrainment coefficient predicts the rate of sediment erosion at a shear stress higher than the critical shear stress.

ii. C_d quantifies the resistance of the sand particles to the fluid flow. Engelund and Hansen (*24*) proposed the following equation for natural sands and gravels based on laboratory measurements:

$$C_d = \frac{24}{R_e} + 1.5 \qquad (4)$$

For a large Reynolds number signifying turbulent flow, the C_d is approximately equal to 1.5.

iii. C_b is related to the transport of heavy particles along the top of the packed bed by the flow of water. In this process, the bed load coefficient is used to predict the rate of transport at a shear stress higher than the critical shear stress. The default value of the bed load coefficient is 8.0 in FLOW-3D (*21*) following the Meyer-Peter and Muller (*25*) equation. Nnadi and Wilson (*26*) reported a C_b value of 12 for a sheet flow regime, and Ribbernik (*27*) suggested a C_b of 5.7 for bed load data that are very close to the incipient motion. A typical C_b for sand and gravel is 5.7 (*27, 28*).

Table 1 provides values of the different parameters used for sandy soil. These value ranges are used as input parameters in the sediment scour model. As explained earlier, the 'Critical Shields Parameter' value cell is blank in the table for the numerical simulations because the number is computed from the Shields curve (*23*). The C_d value was varied from 1.0 to 2.0 (*29, 30*), the C_e value was varied from 0.009 to 0.036, and the C_b value was varied from 4 to 8. These ranges are assumed based on consideration of the data found in the literature.

TABLE 1 Numeric Parameter Values Used in Numerical Simulations

Parameter	Value
Density, ρ	1500 Kg/m^3
Critical Shields Parameter	---
Drag Coefficient, C_d	1 to 2
Entrainment Coefficient, C_e	0.009 to 0.036
Bed Load Coefficient, C_b	4 to 8
Angle of Repose, Φ	31º

FLOW-3D has five different turbulence models for simulating turbulent flow: Prandtl's mixing length theory, one-equation turbulent energy (k), two-equation turbulent energy (k-ε), renormalization group (RNG) and the large eddy simulation model. The RNG model is used in this study because it can describe low intensity turbulence flow with strong shear regions more accurately than the other models (*31*) and, in this case, seems to better fit the jetting scheme.

Model Geometry

Similar to the Pea Island bridge site, the modeled bed consists of sand in two layers, with the grain size distributions obtained from the field. As shown in Figure 4, the domain configuration consists of a sand bed that is 30 m long, 20 m wide and 4 m deep. A uniform mesh with 0.50 m spacing was used for the numerical simulation, with a total of 48,392 cells. The *sediment scour* model, *viscosity and turbulence* model and *gravity* model were then activated. The gravity model was activated by specifying the gravity component of 9.8 m/s^2 in the z direction. Fluid flow was induced from the upstream boundary with a specified velocity that was varied from 0.45 m/s to 0.9 m/s with a constant depth of flow of 1.0 m. Two cylindrical piers, 3 m in height from the surface and 1.22 m in diameter, were simulated to assess the local scour. The center-to-center spacing between the piers was 3 m.

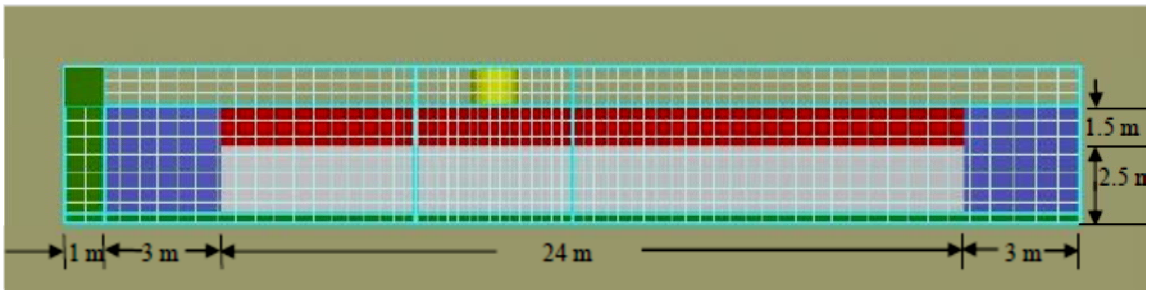

FIGURE 4. Discretized domain for numerical simulation of scour around piers with sand bed and 1 m outfall-side view (Upstream boundary = Green; Top soil layer = Red; Bottom bed = Grey; and Pier = Yellow).

Simulation Results

The flow regime was simulated with time, and the results from the numerical model include data for bed shear stress, the erosion profile, and the maximum erosion depth as a function of flow velocity. Using the bed shear stress data computed from the model, the erosion rate at the pier was calculated using Equation 3 on the basis of the parameters used in the ISEEP field testing.

Effect of Model Parameters

Figure 5 presents a comparison between the maximum scour depth measurements obtained based on the ISEEP parameters and the values computed using FLOW-3D, with a range of the C_e, C_b, and C_d parameters. Figures 5a, 5b and 5c present the simulated and computed scour depths obtained from both approaches. The excess shear stress value (therefore the stream power) was varied by changing the applied velocity in the upstream channel. The flow velocity was varied from 0.45 m/s to 0.9 m/s, which corresponds to stream power values in the range of 125 watt/m^2 to 850 watt/m^2. The C_e, C_b, and C_d values used for estimating the shear stress, and to use in conjunction with the ISEEP data, are 0.018, 5.7, and 1.5, respectively. These values are most commonly specified for sand (*32, 27, 24*) and are within the range of values specified in Table 1.

Figure 5a shows the effect of the entrainment coefficient, C_e, on the computed scour depth and as a function of stream power. The C_e was varied from 0.009 to 0.036. The figure shows that as the C_e value increases, the scour depth also increases. It is of interest to note that the maximum scour depth for C_e is 0.009, whereas such a limit was not reached for the C_e value of 0.036 within the range of stream power values used in the analysis. Mastbergen and Von den Berg (*32*) indicated that the rate of erosion is linearly proportional to the entrainment coefficient. However, such a linear trend is not observed in Figure 5a. For example, the depth of scour increases 70% for $C_e = 0.036$ versus $C_e = 0.009$ at a stream power = 600 watt/m^2.

Figure 5b shows the effect of the drag coefficient, C_d, on scour depth. With an increase in the C_d, the magnitude of the scour depth decreases. The C_d value represents the resistance of the sand particles to the fluid flow and thus the observed reduction in the maximum scour depth under the same stream power value with an increasing C_d. At a stream power value of 600 watt/m^2, the depth of scour decreases by 25% when the C_d is doubled.

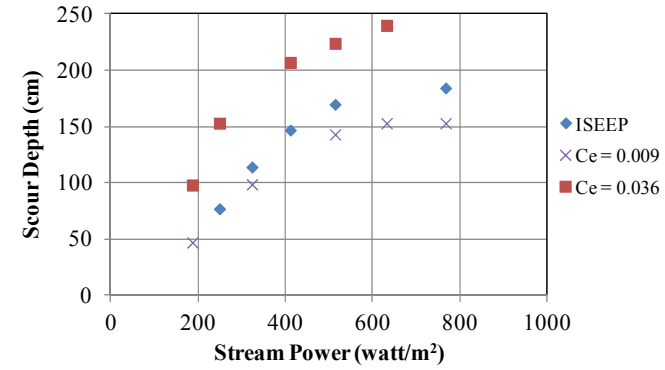

(a)

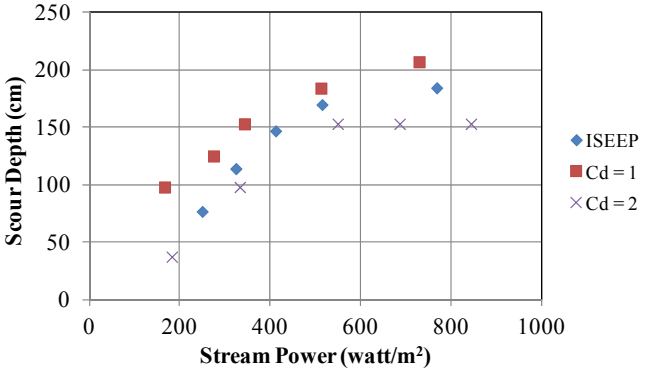

(b)

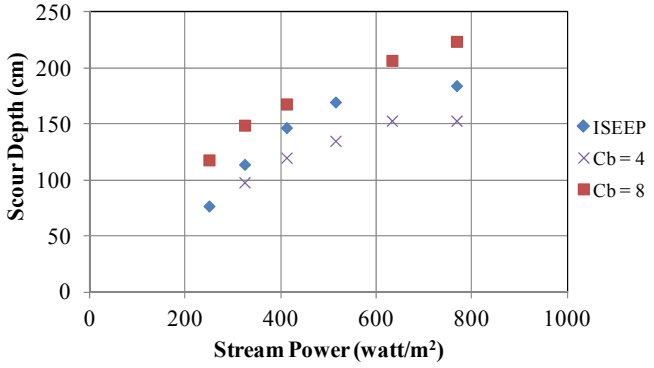

(c)

FIGURE 5. Comparison of maximum scour depth around bridge piers versus stream power obtained from ISEEP tests and different (a) entrainment coefficients, (b) drag coefficients and (c) bed load coefficients.

Figure 5c shows the effect of the bed load coefficient, C_b. The C_b parameter reflects the rate of bed load transport relative to the critical shear stress, and was varied from 4 to 8. Figure 5c shows that with an increase in the C_b value, the depth of scour increases. At a stream power value of 600 watt/m^2, the depth of scour increases by 25% when the C_b is doubled. As presented by Ribberink (*27*), the transport of heavy particles from the top of the bed in the direction of the fluid flow increases with higher C_b values and, therefore, the scour depth increases.

The results of the analyses indicate that among the three input parameters, the entrainment coefficient has the largest effect on scour depth, whereas the drag coefficient has the

smallest effect. Figures 5a, 5b and 5c, also show that the computed scour depth measurements based on ISEEP data are within the values obtained from the FLOW-3D results, with the best match observed for the case of C_e, C_b and C_d values of 0.018, 5.7 and 1.5, respectively.

COMPARISON WITH EMPIRICAL EQUATIONS

Various approaches exist for empirically assessing bridge pier scour. Melville and Sutherland (*12*) suggested a maximum scour depth (d_s) to pier diameter (b) ratio of 2.4 in laboratory flume tests. Ettema (*33*) found that depth of scour becomes independent of depth of flow (y) when the depth of flow to pier diameter ratio is greater than 3. Table 2 shows empirical equations to estimate the maximum scour depth in sandy soil; these equations have a provision for flow velocity and, therefore, can be used for comparison with results obtained from the numerical analyses and ISEEP predictions.

TABLE 2 Empirical Equations to Estimate Local Scour around Bridge Piers

Reference	Equation	Comments
Shen et al. (*11*)	$d_s = 0.000223\ (Vb/\upsilon)^{0.619}$	V = flow velocity, υ = kinematic viscosity of water = 1×10^{-6} m^2/s
Richardson and Davis (*14*)	$d_s/b = 2K_sK_{theta}K_3K_4(y/b)^{0.35}Fr^{0.43}$	K_s = shape factor, K_{theta} = inclination factor, K_3 = factor for mode of sediment transport, K_4 = factor for armoring by bed material, Fr = Froude number
Breusers et al. (*34*)	$d_s/b = f\ (V/V_c)(2\tanh(y/b))K_sK_{theta}$	$f\ (V/V_c) = 0,\ V/V_c \leq 0.5$ $= (2V/V_c - 1),\ 0.5 < V/V_c \leq 1$ $= 1,\ V/V_c > 1$ V_c = Critical velocity
Jain and Fischer (*35*)	$d_s/b = 1.86(y/b)^{0.5}(Fr - Fr_c)^{0.25}$	Fr_c = Critical Froude Number

Other empirical equations by Laursen and Toch (*10*), Melville and Sutherland (*12*), and Melville (*36*) were developed on the basis of only depth of flow and geometric dimensions. Therefore, these equations are not used in this study because comparisons with ISEEP-evaluated scour are not possible. Table 3 presents the input parameters and factors that are required to calculate scour depth using the empirical equations in terms of the methodology used to estimate the input parameters.

Figure 6 presents a comparison of scour depth normalized by the pier diameter, using empirical equations, FLOW-3D, and based on ISEEP data. The stream power is varied by changing the flow velocity from 0.5 m/s to 0.9 m/s. Figure 6 indicates that the simulated and computed scour depths obtained from both ISEEP and FLOW-3D agree relatively well. However, with an increase in stream power, the estimated scour magnitude values derived from ISEEP and FLOW-3D divert from the values estimated using the empirical equations. The difference in scour depth increases with the increase in flow velocity, i.e., stream power. For a stream power value of 400 watt/m^2, the difference of scour depth to the pier diameter ratio is approximately 25% based on results from the empirical equations versus those assessed based on ISEEP data. This difference increases to 50% when the stream power nearly doubles, with the magnitude of scour depth under-predicted by the empirical equations.

TABLE 3 Parameters Used in the Empirical Equations

Parameter	Comments
V_c = Critical velocity	Calculated using $V_c/u_{*c} = 5.75 \log (5.53y/d_{50})$, where shear velocity $u_{*c} = 0.03(d_{50})^{1/2}$ and y = depth of flow (*12*)
Fr = Froude number	$Fr = V/(gy)^{0.5}$, where V is flow velocity and g is gravitational acceleration
K_s = shape factor	$K_s = 1$ for circular piers (*12*)
K_{theta} = inclination factor	$K_{theta} = 1$ for angle of attack 0 degree (*12*)
K_3 = factor for mode of sediment transport	From Richardson and Davis (*14*), when $V/V_c > 1$ the scour in the channel bed is live-bed scour (which is the movement of the bed material from the upstream to the pier hole) and $K_3 = 1$.
K_4 = factor for armoring by bed material	According to Richardson and Davis (*14*), for a $d_{50} < 2$ mm $K_4 = 1$. This study was performed with $d_{50} = 0.32$ mm. Therefore $K_4 = 1$.

The difference in the estimated depths of scour may be explained by the fact that the results based on the ISEEP data and FLOW-3D account for two layers soil system, whereas the empirical equations have been developed for a single-layer system and did not explicitly include soil properties in the equations. By the time the scour depth exceeds 1.5 m, the grain size distribution of the looser sand in the second layer controls the rate and, therefore, the difference.

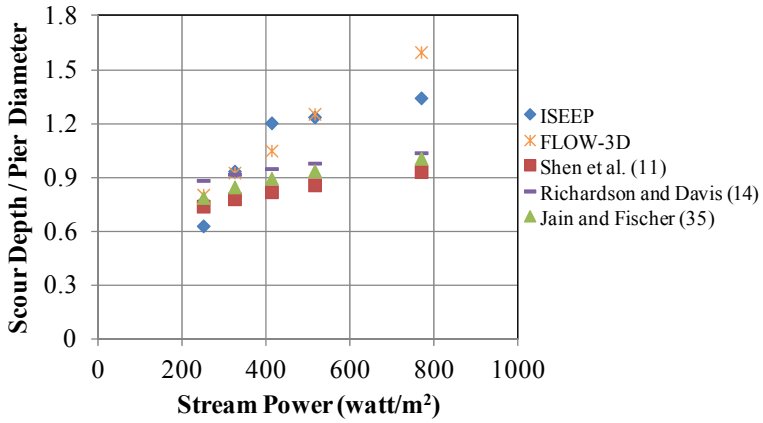

FIGURE 6. Scour depth to pier diameter ratio vs. stream power for ISEEP data and FLOW-3D using empirical equations from the literature.

SUMMARY AND CONCLUSIONS

This paper presents a case study that illustrates the use of an *in situ* device, termed ISEEP, which is used to assess the scour potential in terms of depth at a bridge site. The CFD software, FLOW-3D, is used to study the potential scour magnitude at a bridge pier with soil properties obtained from a site at a North Carolina Outer Banks site where a breach occurred during Hurricane Irene in 2011. The variations in scour depth with the change in flow velocity (i.e., stream power) is examined by varying the drag, entrainment, and bed load coefficients. Based on field test results, the detachment rate coefficient and the critical stream power are estimated using ISEEP test data. The bed shear stress values are obtained from FLOW-3D analyses, and the scour depth is calculated based on ISEEP data using an excess stream power approach. Based on the parameters and findings of this study, the following observations are advanced:

1. The rate of probe advancement is correlated to jet velocity, and erosion parameters are provided for two subsurface layers. The data reduction approach illustrates the viability of defining soil erosion parameters in terms of critical stream power and modified detachment rate coefficients for the two-layer system at the test site.
2. The parametric analyses indicate that among the parameters commonly used to define scour depth, the entrainment coefficient has the largest effect and the drag coefficient has the smallest effect on the estimated scour depth.
3. The scour depths estimated using ISEEP parameters agree relatively well with values obtained from the 3-D numerical analyses, as these estimates were obtained by accounting for the changes in the properties of the subsurface sand layers. The ISEEP-estimated depth measurements best match with those of FLOW-3D for C_e, C_b and C_d values of 0.018, 5.7 and 1.5, respectively.
4. For the case study presented herein, the empirical equations considered in the analysis yield smaller estimates of the scour depth at the pier compared to those from the numerical analysis. These equations do not explicitly account for the variation in soil properties in terms of depth and do not have a provision for a layered soil system or time-dependent scour rate.

The use of ISEEP data provides the advantage of *in situ* testing as well as the potential for estimating the scour parameters because the soil layers vary with depth. Further laboratory and field validations of the proposed test and data reduction approaches are needed. Such validation should include an investigation of the applicability of the approach in soils with appreciable percentages of fines.

ACKNOWLEDGEMENT

The material in this paper is based upon work supported by the U.S. Department of Homeland Security under Award Number 2008-ST-061-ND 0001. The views and conclusions contained in this document are those of the authors and should not be interpreted as necessarily representing the official policies, either expressed or implied, of the U.S. Department of Homeland Security.

REFERENCES

1. Lagasse, P. F., E. V. Richardson, J. D. Schall, and G. R. Price. *Instrumentation for measuring scour at bridge piers and abutments.* National Cooperative Highway Research Program (NCHRP) Report No. 396, Transportation Research Board, Washington, D.C., 1997.
2. Briaud, J. -L., F. C. K. Ting, H. C. Chen, Y. Cao, S. -W. Han, and K. Kawk. Erosion Function Apparatus for Scour Rate Predictions. *Journal of Geotechnical and Geoenvironmental Engineering*, Vol. 127, No. 2, 2001, pp. 105-113.
3. Lu, J. -Y, J. -H. Hong, C. -C. Su, C. -Y. Wang, and J. -S. Lai. Field Measurements and Simulation of Bridge Scour Depth Variations during Floods. *Journal of Hydraulic Engineering*, Vol. 134, No. 6, 2008, pp. 810-821.
4. Hanson, G. J., K. M. Robinson, and K. R. Cook. Scour Below an Overfall: Part II. Prediction. *Transactions of the American Society of Agricultural Engineers*, Vol. 45, No. 4, 2002, pp. 957-964.

5. Hanson, G. J., and K. R. Cook. Apparatus, Test Procedures, and Analytical Methods to Measure Soil Erodibility In Situ. *Applied Engineering in Agriculture*, Vol. 20, No. 4, 2004, pp. 455-462.
6. Mehta, A. J. Review Notes on Cohesive Sediment Erosion. In *N.C. Kraus, K.J. Gingerich, and D.L. Kriebel, (eds.), Coastal sediment '91, Proceedings of Specialty Conference on Quantitative Approaches to Coastal Sediment Processes*, 1991, pp. 40– 53.
7. Annandale, G.W. *Scour Technology: Mechanics and Practice*. McGraw Hill, New York, 2006.
8. Gabr, M., C. Caruso, A. Key, and M. Kayser. Assessment of In Situ Scour Profile in Sand using a Jet Probe. Journal article accepted in ASTM.
9. Melville, B.W., and S.E. Coleman. *Bridge Scour.* Water Resources Publications, LLC, USA, 2000.
10. Laursen, E. M. and A. Toch. *Scour around Bridge Piers and Abutments*. Bulletin No. 4, Iowa Highway Research Board, 1956.
11. Shen, H. W., V. R. Scheider, and S. Karaki. Local Scour around Bridge Piers. *Journal of Hydraulic Engineering*, Vol. 95, No. 6, 1969, pp. 1919-1940.
12. Melville, B.W., and A.J. Sutherland. Design Method for Local Scour at Bridge Piers. *Journal of Hydraulic Engineering*, Vol. 114, No. 10, 1988, pp. 1210-1227.
13. Melville, B.W. *Local Scour at Bridge Sites*. Report No. 117, University of Auckland, School of Engineering, Auckland, New Zealand, 1975.
14. Richardson, E. V., and S. R. Davis. *Evaluating Scour at Bridges*. Rep. No. FHWA-IP-90-017, Hydraulic Engineering Circular No. 18 (HEC-18), 3rd Ed., Office of Technology Applications, HTA-22, Federal Highway Administration, U.S. Dept. of Transportation, Washington, D.C., 1995.
15. Mueller, D. S. *Local Scour at Bridge Piers in Nonuniform Sediment under Dynamic Conditions*. Ph.D. thesis, Colorado State University, Fort Collins, CO, 1996.
16. Richardson, J. E., and V. G. Panchang. Three-Dimensional Simulation of Scour Inducing Flow at Bridge Piers. *Journal of Hydraulic Engineering*, Vol. 124, No. 5, 1998, pp. 530-540.
17. Ali, K. H. M., and R. Karim. Simulation of Flow around Piers. *Journal of Hydraulic Research*, Vol. 40, No. 2, 2002, pp. 161-174.
18. Salaheldin, T. M., J. Imran, and M. H. Chaudhry. Numerical Modeling of Three Dimensional Flow Field around Circular Piers. *Journal of Hydraulic Engineering*, Vol. 130, No. 2, 2004, pp. 91-100.
19. Roulund, A., B. M. Sumer, J. Fredsoe, and J. Michelsen. Numerical and Experimental Investigation of Flow and Scour around a Circular Pile. *Journal of Fluid Mechanics*, Vol. 534, 2005, pp. 351-401.
20. Kurum and Overton. (2012). Personnel communication.
21. FLOW-3D (2011). *User Manual*. Flow Science, Inc.
22. Hirt, C., and J. Sicilian. A Porosity Technique for the Definition of Obstacles in Rectangular Cell Meshes. In *Proc. Fourth International Conf.*, Ship Hydro., National Academy of Science, Washington, D.C., 1985.
23. Brethour, J., and J. Burnham. Modeling Sediment Erosion and Deposition with the FLOW-3D Sedimentation & Scour Model. *Flow Science Technical Note*, FSI-10-TN85, 2010, pp. 1-22.

453 24. Engelund, F., and E. Hansen. A Monograph on Sediment Transport to Alluvial Streams.
454 Copenhagen, Tenik Vorlag, 1967.
455 25. Meyer-Peter, E. and R. Mueller. Formulas for Bed-Load Transport. In. *Proc*. Second
456 Meeting of the International Association for Hydraulic Research, *IAHR*, *Stockholm*,
457 Sweden, 1948, pp. 39-64.
458 26. Nnadi, F. N., and K. C. Wilson. Motion of Contact-Load Particles at High Shear Stress.
459 *Journal of Hydraulic Engineering*, Vol. 118, No. 12, 1992, pp.
460 27. Ribberink, J. S. Bed-Load Transport for Steady Flows and Unsteady Oscillatory Flows.
461 *Coastal Engineering*, Vol. 34, 1998, pp. 59– 82.
462 28. Fernandez, L. R., and R. Van Beek. Erosion and Transport of Bed-Load Sediment. *Journal*
463 *of Hydraulic Research*, Vol. 14, No. 2, 1976, pp. 127-144.
464 29. Rubey, W. Settling Velocities of Gravel, Sand and Silt Particles. *American Journal of*
465 *Science*, Vol. 25, No. 148, 1933, pp. 325–338.
466 30. Wu, W., and S. S. Y. Wang. Formulas for Sediment Porosity and Settling Velocity.
467 *Journal of Hydraulic Engineering*, Vol. 132, No. 8, 2006, pp. 858-862.
468 31. Yakhot, V., and S.A. Orszag. Renormalization Group Analysis of Turbulence. I. Basic
469 Theory. *Journal of Scientific Computing*, Vol. 1, No. 1, 1986, pp. 3–51.
470 32. Mastbergen, D. R., and J. H. Van den Berg. Breaching in Fine Sands and the Generation of
471 Sustained Turbidity Currents in Submarine Canyons. *Sedimentology*, Vol. 50, No. 4, 2003,
472 625-637.
473 33. Ettema, R. *Scour at bridge piers*. Report No. 216, Dept. of Civil Engineering, University of
474 Auckland, Auckland, New Zealand, 1980.
475 34. Breusers, H. N. C., G. Nicollet, and H. W. Shen. Local Scour around Cylindrical Piers.
476 *Journal of Hydraulic Research*, Vol. 15, No. 3, 1977, pp. 211-252.
477 35. Jain, S. C., and E. E. Fischer. *Scour around Bridge Piers at high Froude Numbers*. Report
478 Number FHWA-RD-79-104, Federal Highway Administration, Washington D.C., 1979.
479 36. Melville, B. W. Pier and Abutment Scour—An Integrated Approach. *Journal of Hydraulic*
480 *Engineering*, Vol. 123, No. 2, 1997, pp. 125–136.
481